Chapter 8

Analysis of the Influence of Fish Behavior on the Hydrodynamics of Net Cage

Tiao-Jian Xu, Ming-Fu Tang and Guo-Hai Dong

Additional information is available at the end of the chapter

http://dx.doi.org/10.5772/intechopen.71015

Abstract

In net cage hydrodynamic analysis, drag force of net is dependent on the physical dimensions of the net cage, the Solidity ratio, the Reynolds number and the projected area of the net, which is illustrated in numerous previous researches. However, rare studies attempt to investigate the effect of fish behavior. Thus a net-fluid interaction model and a simplified fish model were proposed for analyzing the effects of fish behavior on the net cage. A series of physical model tests were conducted to validate the numerical model, which indicates models can simulate the stocked net cage in the current accurately. The simulation results indicate that circular movement of fish leads to a low pressure zone at the center of net cage, which causes a strong vertical flow along the center line of the net cage. The drag force on the net cage is significantly decreased with the increasing fish stocking density.

Keywords: SST k-omega model, finite element method, net cage, fish behavior

1. Introduction

A slew of researches show that the drag force (F_D) on a net cage is dependent on the physical dimensions of the net cage, the Solidity ratio, the Reynolds number and the projected area of the net. In addition, the fish behavior, such as the fish distribution, the fish swimming velocity and the fish group structure, plays a significant role in the net cage hydrodynamic analysis. Based on the previous site observation in the commercial net cage, Gansel discovered a strong diurnal variation of the fish distribution, indicating that most fishes at night were near the top of net cage, while majorities of fish during daytime were near the bottom of net cage [1]. According to the recent observations on the Atlantic salmon swimming behavior at a commercial farm, Johansson proposed that at the low current velocities (<0.45 BL/s, BL: fish body length), salmon

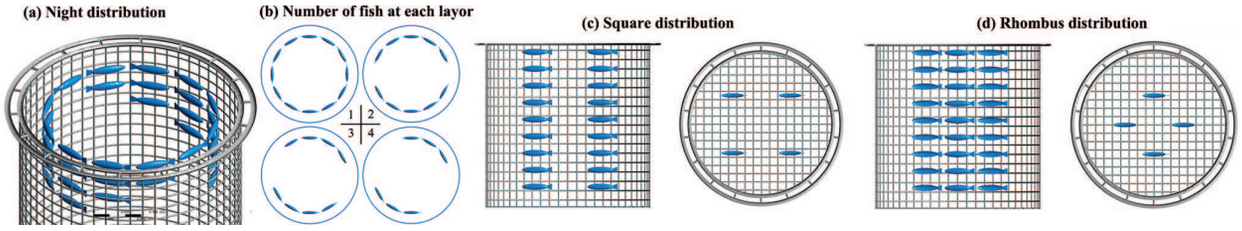

Figure 1. Fish group structure in this chapter (a-d).

group polarized swam in a circular movement and at the high current velocities (>0.90 BL/s), all fishes kept stations at fixed positions swimming against the current [2].

In this chapter, two types of fish distribution patterns were analyzed: night distribution, fish is mainly gathered in the water surface and fish density is decreased with increasing water depth; and day distribution, most fishes perched near to the bottom of net cage and fish density is increased with increasing water depth. And two kinds of fish group structures are considered: circular (**Figure 1**) = polarized swimming in a circular movement; on-current (**Figure 1**) = swimming toward the current without forward movement. The latest progress of net cage numerical simulation method by our research group will be introduced in detail. The contents of the progresses include the following parts: *The introduction of an elaborate net cage model and fish model; The validation of models in steady flow; The numerical simulation of the stocked net cage in steady flow.*

2. Numerical modeling approach

The numerical modeling for analyzing the flow field through the stocked net cage and the deformation of net cage is to combine the *k-ω* Shear Stress Turbulent (SST) model and the large deformation nonlinear structure (LDNS) model. In the combined analysis, the two methods are handled separately.

2.1. Flow around net cage

The *k-ω* SST model, developed by Menter in [3], is applied to simulate the flow filed around the net cage structure.

2.1.1. The k-ω SST model

The governing equations describing the *k-ω* SST turbulence model are as follows:

Continuity equation:

$$\frac{\partial \rho}{\partial t} + \frac{\partial (\rho u_i)}{\partial x_i} = 0 \tag{1}$$

Momentum equation:

$$\frac{\partial(\rho u_i)}{\partial t} + \frac{\partial(\rho u_i u_j)}{\partial x_j} = \frac{-\partial P}{\partial t} + \rho g_i + \frac{\partial}{\partial x_j}(\mu + \mu_t)\left(\frac{\partial u_i}{\partial x_j} + \frac{\partial u_j}{\partial x_i}\right) \tag{2}$$

where ρ is the density of the fluid, u_i and u_j are the time-averaged velocity components for x, y and z, and μ and μ_t are the viscosity of the fluid and the eddy viscosity, respectively. $P = p + (2/3)\rho k$, where p is the time-averaged pressure and P is the transient pressure; k is the turbulent kinetic energy; g_i is the acceleration due to gravity, and $i, j = 1, 2, 3$ (x, y, z).

The k-ω SST model solves two transport equations: the turbulent kinetic energy k and the turbulent dissipation rate ω, as follows:

$$\frac{\partial(\rho k)}{\partial t} + \frac{\partial(\rho u_i k)}{\partial x_i} = \tilde{P}_k - \beta^* \rho k \omega + \frac{\partial}{\partial x_i}\left[(\mu + \sigma_k \mu_t)\frac{\partial k}{\partial x_i}\right] \tag{3}$$

$$\frac{\partial(\rho \omega)}{\partial t} + \frac{\partial(\rho u_i \omega)}{\partial x_i} = \alpha \rho S^2 - \beta \rho \omega^2 + \frac{\partial}{\partial x_i}\left[(\mu + \sigma_\omega \mu_t)\frac{\partial \omega}{\partial x_i}\right] + 2(1 - F_1)\rho \sigma_{\omega 2}\frac{1}{\omega}\frac{\partial k}{\partial x_i}\frac{\partial \omega}{\partial x_i} \tag{4}$$

2.1.2. Boundary conditions

The boundaries of the numerical flume are constituted by a free surface, three wall surfaces, an inlet surface and an outlet surface. The fsi_wall is modeled as a non-slip wall with considering the roughness of the net twine. To consider the roughness of the surface of the actual net twine, the physical roughness height K_s is set as 0.3 mm and the roughness constant C_s is set as 0.5. $y^+ = 1$ is used to determine the thickness of boundary layer.

The governing equations for describing the flow field are solved by a three-dimensional pressure-based Navier-Stokes solver. The SIMPLEC algorithms in [4] are employed to treat the pressure-velocity coupling. The discretization scheme for pressure, momentum, turbulent kinetic energy is carried out using a second order upwind scheme.

2.2. Structural model

The three-dimensional net cage is divided into discrete elements, which the net mesh is modeled as the bar element connected with spherical hinge, as shown in **Figure 2**. The connection force between the net bar and the spherical hinges including two parts: the tangential force and the normal force.

2.2.1. Large deformation nonlinear structure model

The flexible fish net will experience geometric-nonlinear deformation under the action of the hydrodynamic loads, thus the LDNS model (in [5]) is applied here to describe the deformation of flexible fish net. The connection constraints are given as follows:

$$e_j^0 x_i - E_j(X_{c_0} - X_i) = 0 (i = 1, 2, 3; j = x, y, z) \tag{5}$$

where a local Cartesian coordinate, x_0-y_0-z_0, is defined at the center of spherical hinge, c_0, and the coordinate system X-Y-Z is the reference coordinate in the LDNS model as shown in

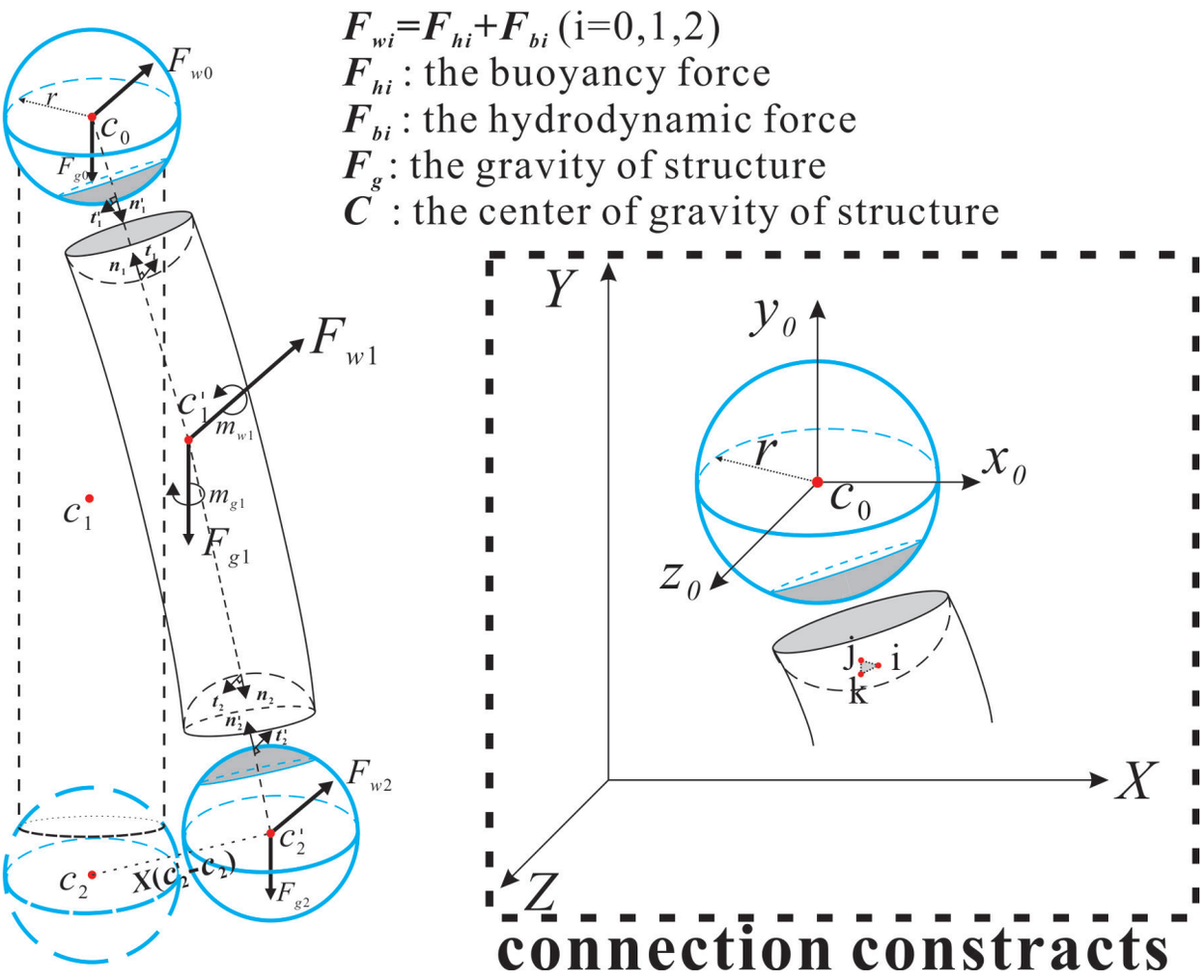

Figure 2. The finite element model of net twine with spherical hinges and mesh bar.

Figure 2; e_j^0, is the unit vector of the local coordinate system C_0-$x_0y_0z_0$ and E_j is the unit vector of the reference coordinate X-Y-Z; the governing equation applied to the LDNS model is given as:

$$[K(x)]x = F_h + F_b + F_g = Q \tag{6}$$

where $K(x)$ is the nonlinear structural stiffness matrix which is related with the unknown displacement vector x.

2.2.2. Load transfer and grid generation

To transfer pressure data from the flow model to the structural model, all nodes on the net twines surface are projected to the fsi_wall element in the flow model according to the mapping rule—projecting each nodes in the target surface normal to the nearest mesh face in the source surface as shown in **Figure 3**. The transferred variable is linearly interpolated on the source face by linear two-dimensional shape function.

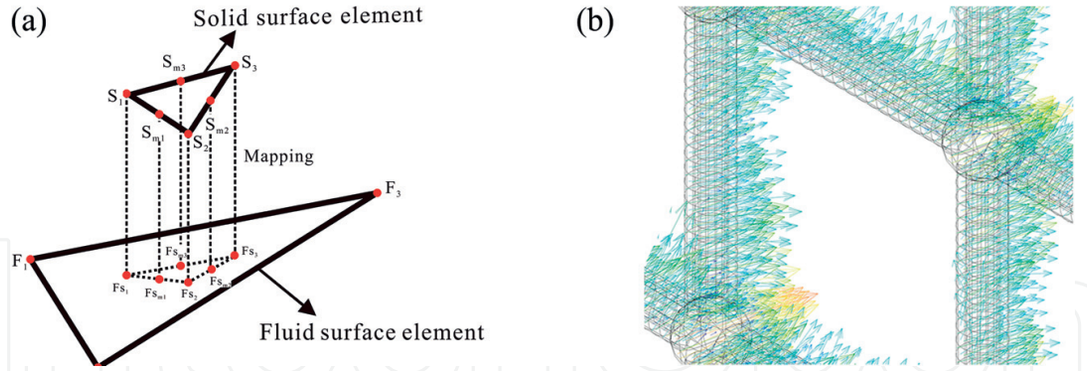

Figure 3. The process of force transfer from fluent solver to structure solver: (a) the sketch of data transfer procedure; (b) the transfer of hydrodynamic force on the net mesh.

2.3. Fish model

As shown in **Figure 4**, the fish model includes the fish body and the fish tail. The fish body suffers the drag force and the fish tail creates the propulsion force. The resulting force of the model includes the propulsion force and the drag force, given as follows:

$$F_x = F_{hx} - F_D cos\beta + F_L sin\beta = \int_{S_t} \tau_{hx} ds - \int_{S_b} \tau_{dx} ds cos\beta = ma_x \tag{7}$$

$$F_y = F_{hy} - F_D sin\beta - F_L cos\beta = \int_{S_t} \tau_{hy} ds - \int_{S_b} \tau_{dy} ds sin\beta = ma_y \tag{8}$$

where the F_D, F_L and F_h are the drag force, lift force and the propulsion force of the model, respectively; τ_d and τ_h are the wall shear stress on the fish body and tail. According to the research (in [6]), the forces on the fish are calculated as follows:

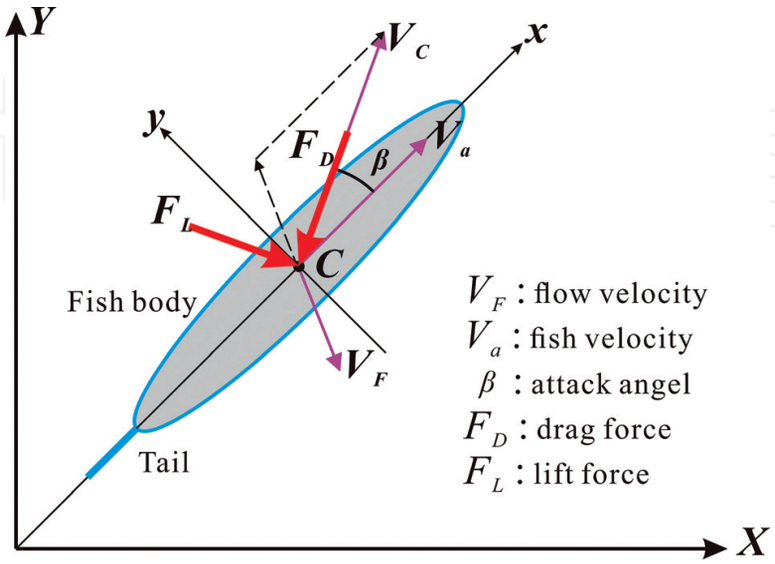

Figure 4. Top view of the tail-actuated fish model.

$$F_D = \frac{1}{2}\rho|V_c|^2 S C_D \, F_L = \frac{1}{2}\rho|V_c|^2 S C_L \tag{9}$$

$$C_D = C_{D0}^{'} + C_{D1}^{'}\alpha_0^2 \, C_L = C_{L\beta}^{'}\alpha_0 = 0.935\alpha_0; \tag{10}$$

where S is the surface area for the fish body, V_c is the relative velocity of fish, β is the attack angle of fish body, C_D and C_L are the drag coefficient and the lift coefficient, $C_{D0}^{'}$ and $C_{D1}^{'}$ are empirical constants equal to 0.1936 and 0.1412 rad^{-2} according to [6], α_0 is the swinging angle of fish tail.

2.4. Grid generation

An example of computational grids for a plane net is shown in **Figure 5(a)**. Tetrahedral grids exist in the majority computational area, and pentahedral prism grids are adopted to refine the meshes near the fluid-solid boundary. Ten boundary mesh layers are adopted to generate boundary grids around fish model as shown in **Figure 5(b)**. Bar elements are divided by hexahedral grids with uniform grid and spherical hinges are divided using tetrahedral grids as shown in **Figure 5(c)**.

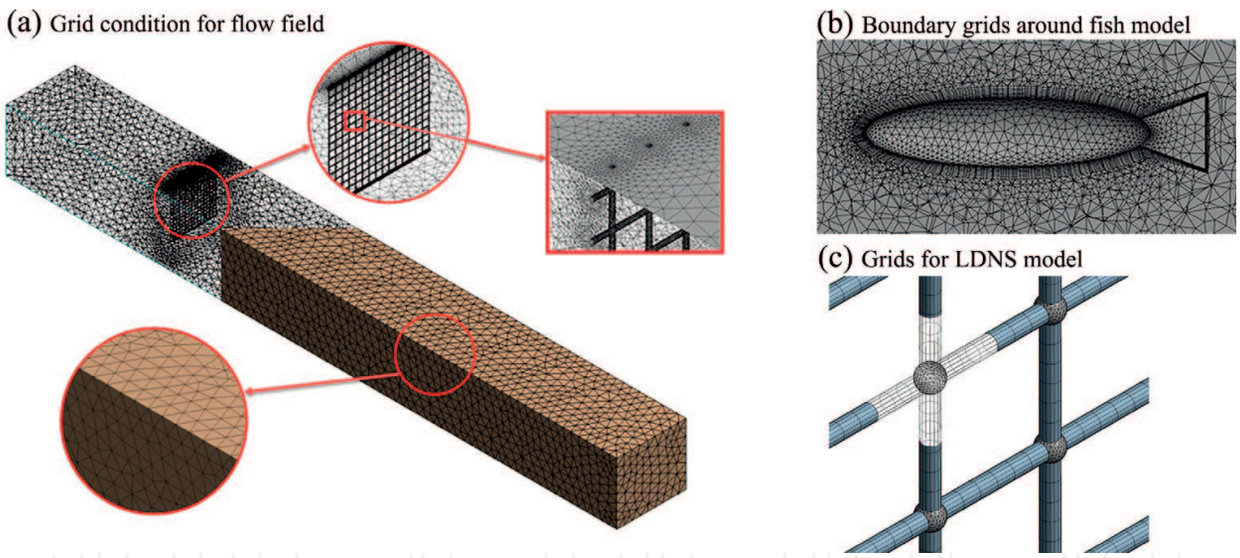

Figure 5. Grid conditions used in this chapter.

3. Experimental validations of model

For fish model validation, a rigid fish model with different behaviors is simulated and the results are compared with the formula proposed in [6]. To validate the net cage model, a series of net cage experiment are conducted a flume at the State Key Laboratory of Coastal and Offshore Engineering, Dalian University of Technology, Dalian, China. The flume is 22 m long, 0.45 m wide and 0.4 m water depth in the tests.

3.1. Validation of the fish model

A single rigid fish model is modeled in the flow as shown in **Figure 6**. The size and weight of fish are same as small fish model (in **Table 1**). The specified wall shear stress in Eqs. (7) and (8), is used to simulate different fish behaviors. There are three operating variables: fish yaw angle, flow velocity and fish swimming velocity, used to investigate the effects of the fish behavior on the flow field and the net deformation. Thus three experiment groups are produced to validate fish model (referring to **Table 2**). **Figure 7** shows that simulation is in good agreement with Eq. (9).

3.2. Validation of the net cage

To validate the deformation of net cage in the steady flow, a net cage model is tested in the flume. The diameter of net cage is 0.254 m and the net mesh is square with 20.0 mm mesh size and 1.2 mm twine diameter. The top of the net is mounted on a top steel ring shown in **Figure 8**.

Figure 9 indicates that the cage deformation simulation is close to the experiment. **Figure 10** indicates the drag force on the net cage from simulation is in good agreement with experiment and the relative error is less than 6.82%.

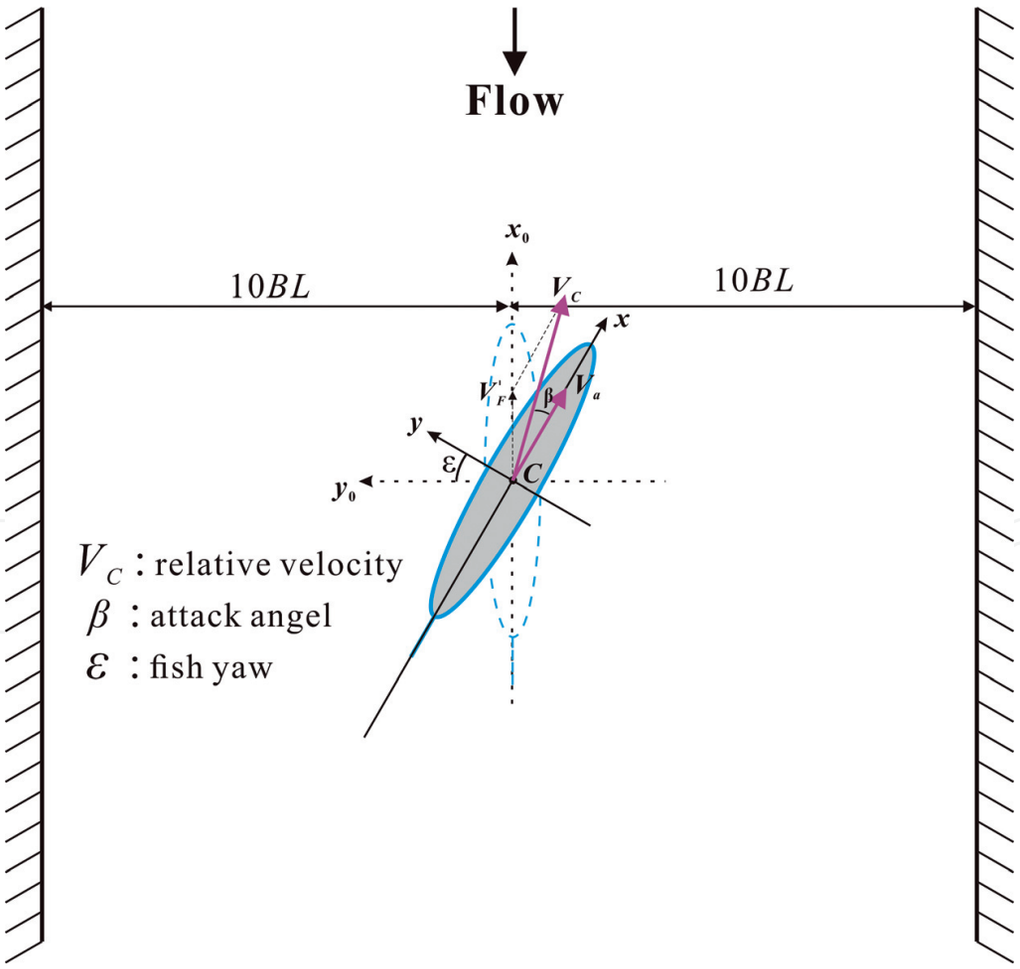

Figure 6. Sketch of the force on single fish model with different yaw in current.

Items	Small fish		Large fish	
	Real fish	Fish model	Real fish	Fish model
Fish length (cm)	40	6.7	50	8.5
Fish surface area (cm^2)	–	1.235	–	2.112

Table 1. The characteristic parameters of fish models applied in the simulation.

No.	V_F (cm/s)	V_a (cm/s)	V_C (cm/s)	Yaw (rad)	β (rad)
1	0	2.0, 3.0, 4.0, 6.0, 8.0, 10.0	2.0, 3.0, 4.0, 6.0, 8.0, 10.0	0	0
2	3.0, 6.0, 6.2	0	3.0, 6.0, 6.2	0	0
3	3.0	6.0	–	0-π	–

***Note*:** V_C and β are determined by fish yaw, flow velocity (V_F) and fish velocity (V_a).

Table 2. Experiment groups of fish model.

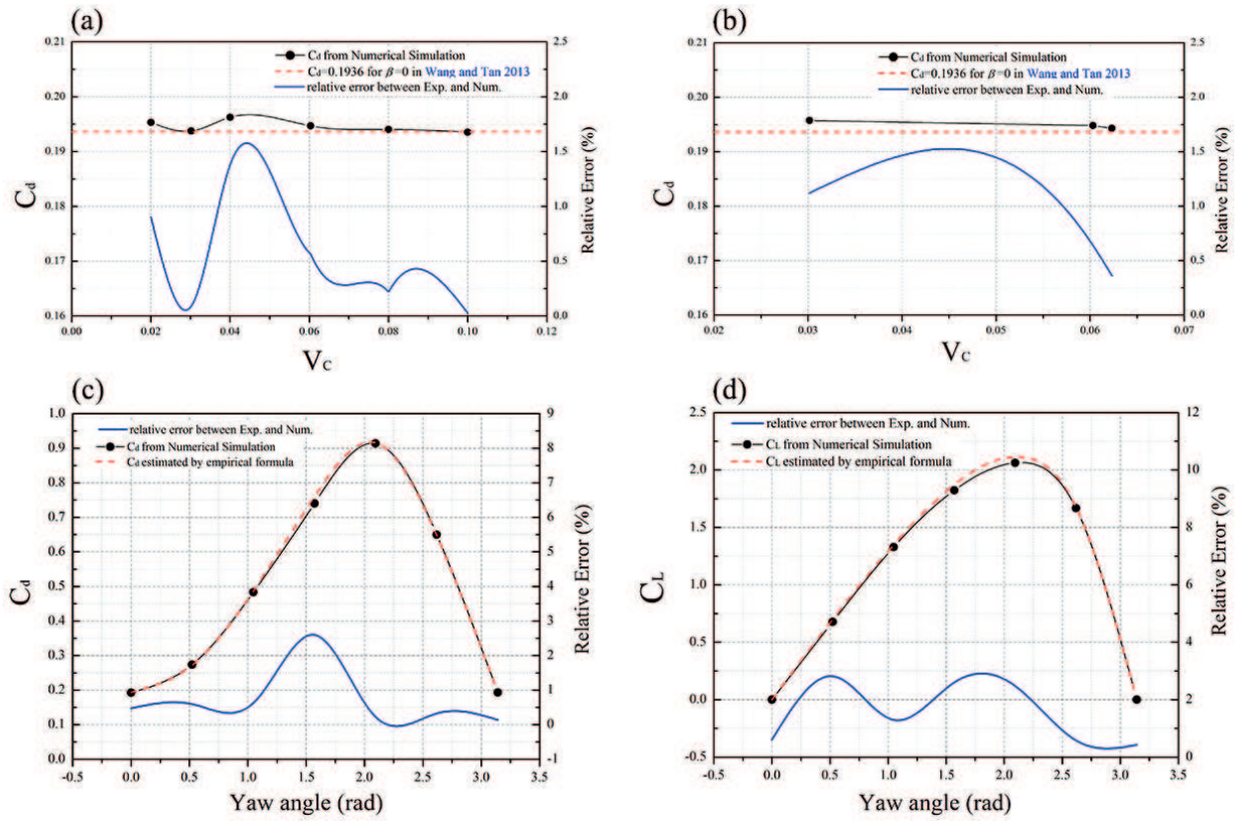

Figure 7. Comparison between simulation and empirical formula: (a) the drag coefficient with different fish velocities in still water; (b) the drag coefficient of fish in different flow velocities; (c) and (d) are the force coefficient of fish for different yaw angles.

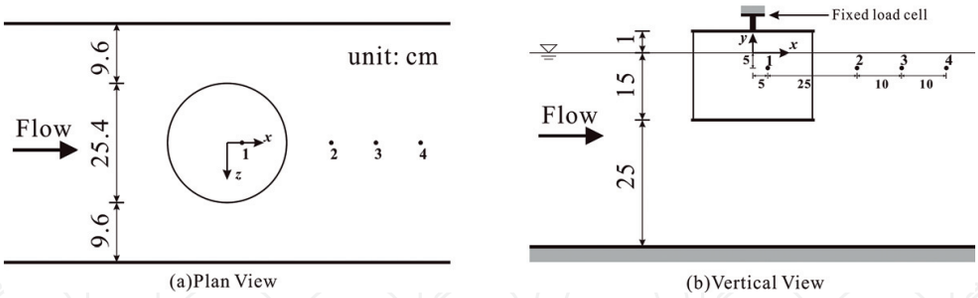

Figure 8. Physical model of net cage and general setting of the measurement points (a, b).

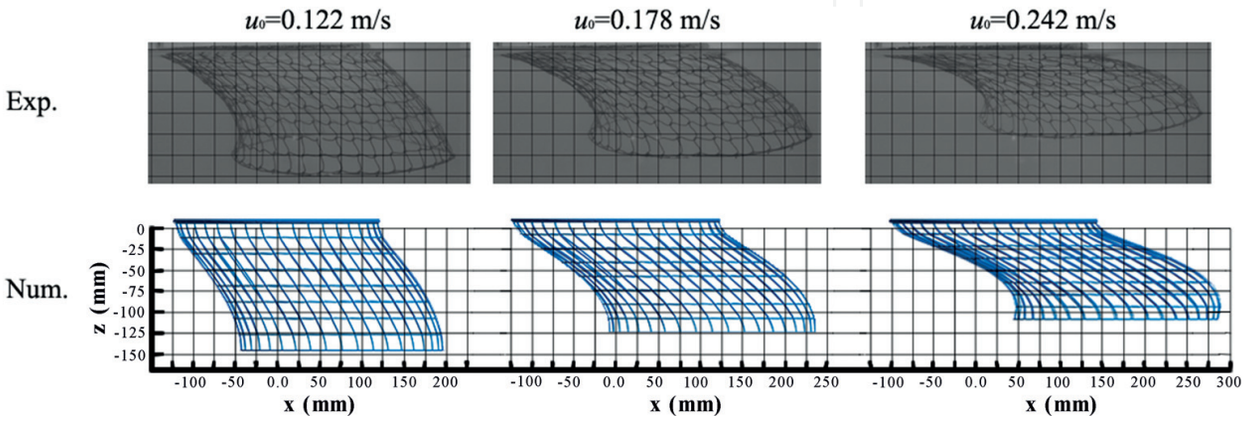

Figure 9. Comparison of the deformation of the net cage between the simulation and experiment.

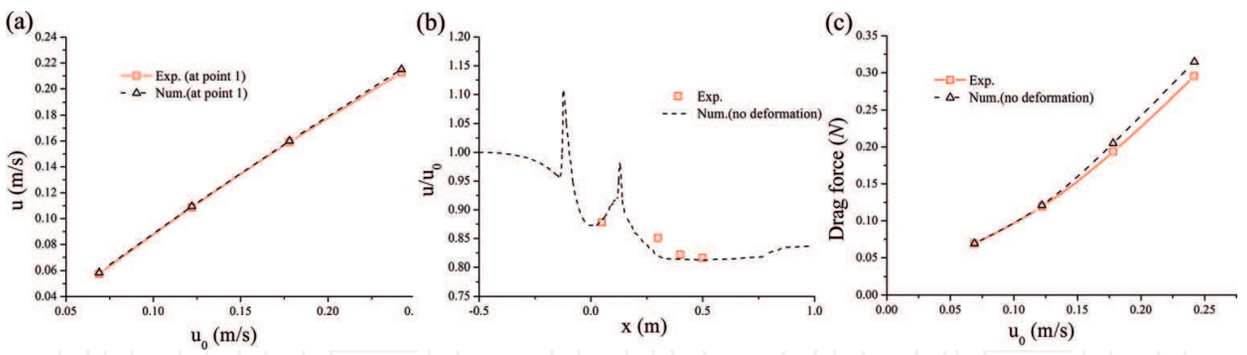

Figure 10. Comparisons of simulation and experiment: (a) flow velocities at point 1 for different incoming velocities; (b) dimensionless flow velocities inside and around net cage with 0.242 m/s incoming velocity; (c) drag forces on net cage for different flow velocities.

4. The numerical simulation of the stocked net cage in steady flow

To investigate the effect of fish behavior on the net cage, a 2.5 m long, 2.5 m wide and 0.7 m depth numerical water flume is adopted here, and the stocked net cage model with 0.35 m outer diameter and 0.35 m height is located at the center of the flume. Sinkers with 1 N weight are applied to maintain the shape of net cage. The net is mounted as square meshes, in which

No.	*SD* (kg/m^3)	Fish model	V_F (BL/s)	Distribution	GS	V_a (BL/s)	A_a (BL/s^2)
1	8	Small	0	Night/day	Circle	0.45 & 0.90 0.45	0 0.45
2	0 8	– Small	0.45	– Night/day	– Circle	– 0.90	– 0
3	0 8	– Small	0.93	– Square/rhombus	– On-current	– 0.93	– 0
4	8 16	Large	0.45	Night/day	Circle	0.90	0
5	24, 32, 40	Large	0.45	Uniform	Circle	0.90	0

BL is the body length of fish; *SD* is stocking density; *GS* is group structure.

Table 3. Experiment groups of fish with different stocking densities and fish distributions.

the twine diameter is 2.6 mm and the mesh bar length is 20 mm. The detailed experiment setup is shown in **Table 3**.

4.1. Circular movement of fish in the still water

The effect of fish swimming on the flow pattern around the net cage in the still water is analyzed, in EG (experiment group) 1 in **Table 3**. **Figure 11** shows the flow pattern in the net cage for different fish distributions with 0.45 BL/s swimming speed. According to Newton's second law, the centripetal force acting on fish need be balanced by the hydrodynamic force which pushes water away from fish. Thus the flow velocity near the inner boundary of fish is greater than that of the outer boundary in the horizontal plane, leading to a low pressure area in the center of the rotational movement of the fish. For the day distribution, water is pulled from above and below the fish swimming depth; for the night distribution, water is only pulled from below the fish swimming depth.

4.2. Effect of fish distribution on flow field and drag force

The effects of fish distribution on the flow field around the net cage and the drag force of the net cage are analyzed in EG 2 and 3. **Figure 12** shows the flow field around the net cage for the low current velocity case (EG 3) and the fish motion in high current case (EG 4) has little influence on

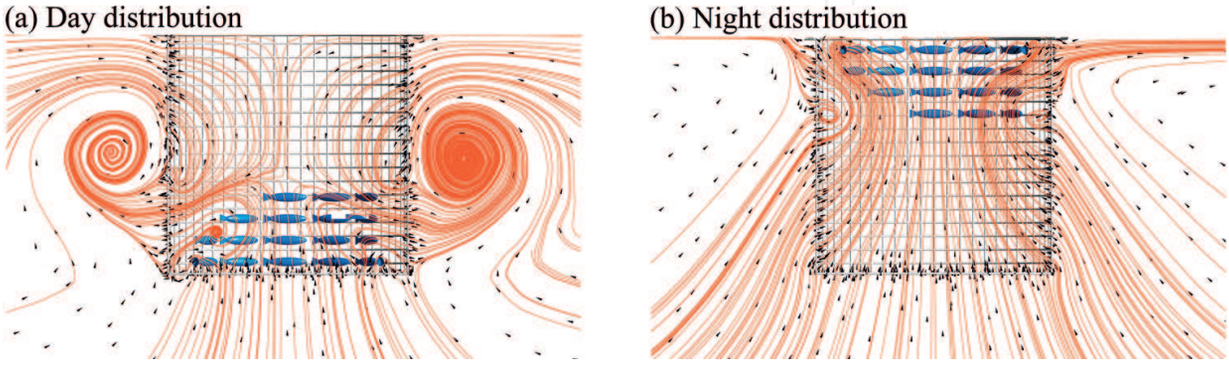

Figure 11. The flow around fish cage for different distributions in still water with 0.45 BL/s fish speed (a, b).

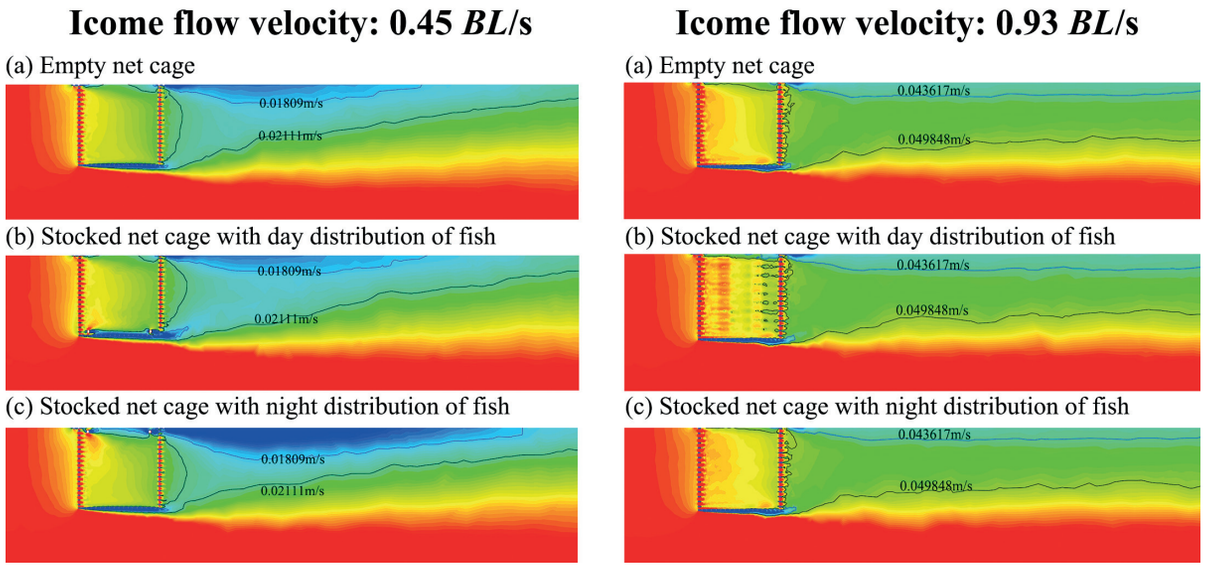

Figure 12. The flow field around the empty net cage and the stocked net cage in low current case (V0 = 0.45 BL/s) and high current case (V0 = 0.93 BL/s) (a-c).

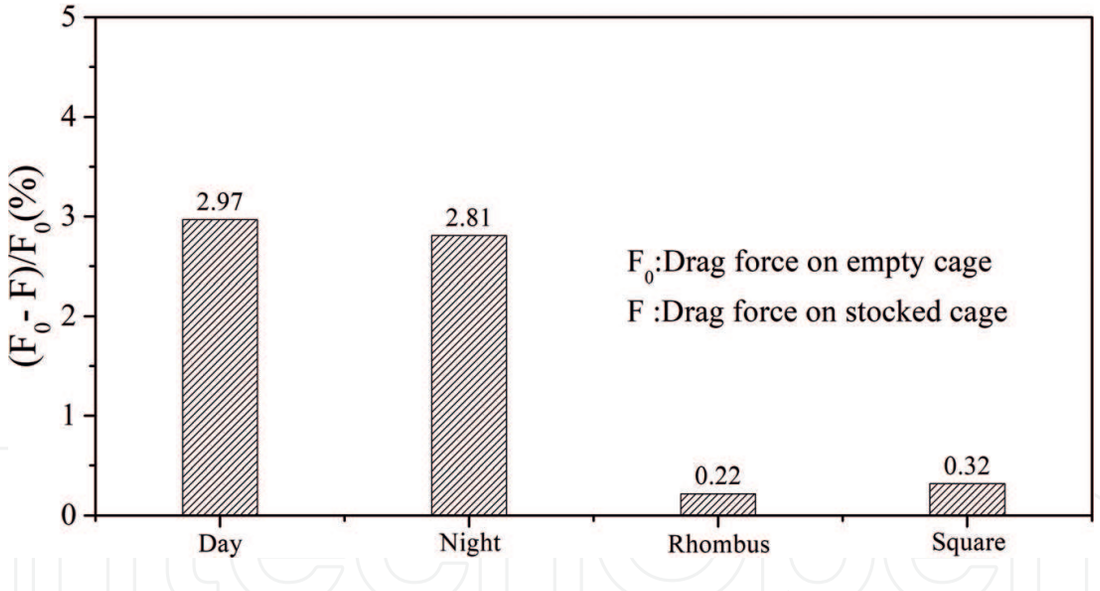

Figure 13. Normalized drag force on the stocked cage for different fish distribution.

the downstream. **Figure 13** shows the circular movement of fish has larger influence on the drag force acting on the net cage and the influence of on-current movement is little.

5. Conclusions

A net-fluid interaction model and a simplified fish model are proposed for analyzing the effects of fish behavior on the flow field around the net cage and the deformation of the net cage. And the following conclusions can be drawn from the case study:

1. The fish circular movement around the net cage can produce a low pressure zone at the center of the net cage, causing a vertical water exchange along the center line of the net cage.
2. The circular movement of fish has significant influence on the downstream wake, and especially the low-velocity zone. While the on-current movements of fishes affect little.
3. The drag force on the net cage is significantly decreased with the increasing fish stocking density. Little differences in the fish distribution are observed.

Acknowledgements

This work was financially supported by the National Natural Science Foundation (NSFC) Projects No. 51239002, 51409037, 51579037, and 51221961, China Postdoctoral Science Foundation (No. 2014M560211 and No. 2015T80254), the Fundamental Research Funds for the Central Universities No. DUT16RC(4)25 and Cultivation plan for young agriculture science and technology innovation talents of Liaoning province (No. 2014008).

Author details

Tiao-Jian Xu*, Ming-Fu Tang and Guo-Hai Dong

*Address all correspondence to: tjxu@dlut.edu.cn

Dalian University of Technology, China

References

[1] Gansel LC, Rackebrandt S, Oppedal F, McClimans TA. Flow fields inside stocked fish cages and the near environment. In: 30-th International Conference on Ocean, Offshore and Arctic Engineering. (OMAE 2011-50205); 2011

[2] Johansson D, Laursen F, FernÖ A, Fosseidengen JE, Klebert P, Stien LH, Vågseth T, Oppedal F. The interaction between water currents and salmon swimming behavior in sea cages. PLoS One. 2014;**9**(5):e97635

[3] Menter FR. Two-equation eddy-viscosity turbulence models for engineering applications. AIAA-Journal. 1994;**32**(8):269-289

[4] Vandoormaal JP, Raithby GD. Enhancements of the SIMPLE method for predicting incompressible fluid flows. Numerical Heat Transfer. 1984;**7**:147-163

[5] Bathe KJ, Ramm E, Wilson EL. Finite element formulations for large deformation dynamic analysis. International Journal for Numerical Methods in Engineering. 1975;**9**:353-386

[6] Wang JX, Tan XB. A dynamic model for tail-actuated robotic fish with drag coefficient adaptation. Mechatronics. 2013;**23**:659-668

IntechOpen

IntechOpen